Journal of the Korean Society of Marine Engineering, Vol. 35, No. 7, pp. 930~937, 2011(ISSN 1226-9549)
http://dx.doi.org/10.5916/jkosme.2011.35.7.930

Turbulence Characteristics in a Circular Open Channel by PIV Measurements

Sun-Gu Kim[1] · Jae-Yong Sung† · Myeong-Ho Lee[2]

(Received November 15, 2011; Revised November 24, 2011; Accepted November 24, 2011)

Abstract : The characteristics of mean velocity and turbulence have been analyzed in the circular open channel flow using PIV measurement data for a wide range of water depth. The measured data are fitted to a velocity distribution function over the whole depth of the open channel. Reynolds shear stress and mean velocity in wall unit are compared with the analytic models for fully-developed turbulent boundary layer. Both the mean velocity and Reynolds shear stress have different distributions from the two-dimensional boundary layer flow when the water depth increases over 50% since the influence of the side wall penetrates more deeply into the free surface. The cross-stream Reynolds normal stress also has considerably different distribution in view of its peak value and decreasing rate in the outer region whether the water depth is higher than 50% or not.

Key words : Circular open channel, Particle image velocimetry, Reynolds stress, Friction velocity, Water depth

1. Introduction

The velocity profile and turbulence characteristics inside a circular pipe are well known, but if the pipe is partially filled, the problem is entirely different since the flow is driven by gravity, not by pressure. The velocity distribution is significantly affected by the pipe slope and water level as well as the wall roughness and surface tension force.

Extensive experiments have been performed on the mean flow and turbulence structure of two-dimensional open channel flow with the help of hot-film anemometers [1-2], laser Doppler anemometers [3-4] and hydrogen-bubble technique [5]. These researches have focused on what differs from the boundary layers of closed channel flows in view of near-wall turbulence. However, unlike the two-dimensional test beds, the circular open channel flow experiences the change of wetted cross-sectional shape as the water depth varies. It means that the side wall may affect the turbulence characteristics and the maximum velocity does not occur at the free surface. The velocity distribution is intrinsically three-dimensional and thus, the traditional approach on the two-dimensional turbulent boundary layer may not valid. For the circular or nonuniform open channel flow, Chiu and his group [6-8] developed a three-dimensional velocity distribution function. However, no systematic analysis of the velocity profile with a wide range of water depth was addressed.

On the other hand, a particle image velocimetry (PIV) [9] has been developed over the last two decades. Doorne and Westerweel [10] successfully applied a stereoscopic PIV technique to the measurement of turbulence in the fully-filled pipe

† Corresponding Author(Dept of Mechanical Engineering, Seoul Tech, Seoul, 139-743 Korea, email:jysung@seoultech.ac.kr)
1 Graduate Student, Dept of Mechanical Engineering, Seoul Tech, Seoul, 139-743 Korea
2 Dept of Mechanical Engineering, Seoul Tech, Seoul, 139-743 Korea

This paper is extended and updated from the short version that apeared in the Proceedings of the International symposium on Marine Engineering and Technology (ISMT 2011), held at BEXCO, Busan, Korea on October 25-28, 2011.

flow. With regard to partially-filled pipe flow (circular open channel flow), Sung et al. [11] measured the three-dimensional velocity profiles using the stereoscopic PIV and the effect of water depth was discussed. However, the turbulence characteristics in the circular open channel flow still need to be investigated.

The purpose of the present study is to analyze the turbulence properties based upon the PIV measurement data in the circular open channel flow. The measurement plane is two-dimensional and located at the axis of symmetry. Experiments are carried out by changing the water depth for a fixed channel slope. The measured mean velocities are fitted to the velocity distribution function. Then, the law of the wall and the Reynolds normal and shear stresses are compared according to the change of the water depth.

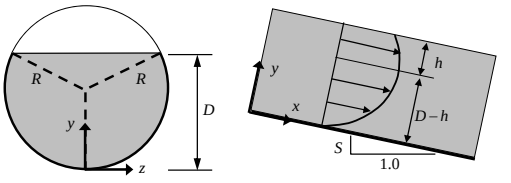

Figure 1: Coordinate system and geometric parameters of the circular open channel flow.

2. Experimental Setup

Figure 1 shows the coordinate system and geometric parameters of the circular open channel flow. An experimental setup to measure the velocity profiles is shown in Fig. 2. A pump provides water through a tube into an influent chamber by regulating discharged flow rate by a valve. At the influent chamber, surplus flow is drained out to the pump inlet. An acrylic test pipe with a radius of $R = 25$ mm and a length of 2.5 m is used for the circular open channel, which is hydrodynamically smooth. The distance between the inlet of the test pipe and the test section is 25 times of the pipe diameter. The water depth is controlled by height adjustment plates installed in both the influent and effluent chambers. The slope of the test pipe can be controlled by a screw jack installed beneath the effluent chamber with the influent chamber being fixed by a hinge. In the present study, the slope is set to be $S = 0.00467$. The water depth D is varied from 30% to 80% with a 10% interval of the pipe diameter of 50 mm.

For the PIV measurements, the test section is made of the acrylic block of a hexahedron to look

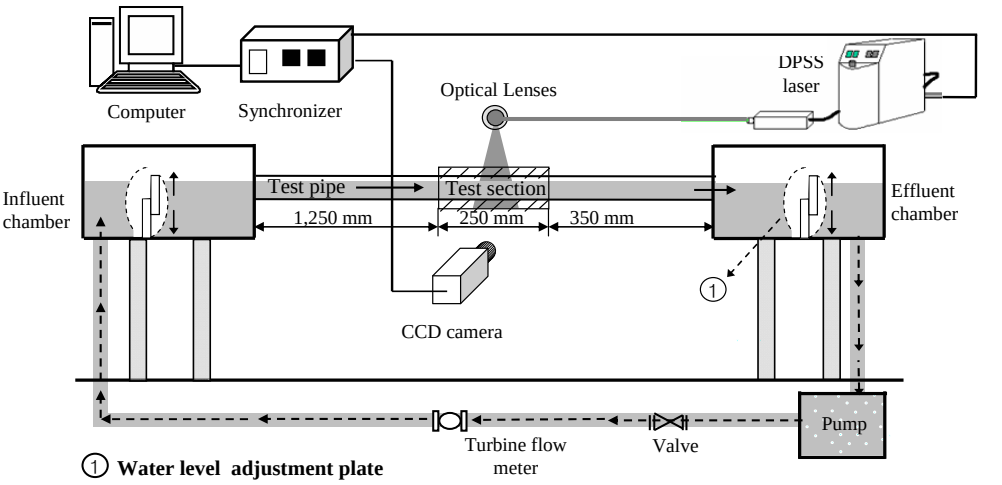

Figure 2: Experimental setup for measuring the circular open channel flow.

transparent. A laser light emitted from an 8W DPSS laser (Blitz) is illuminated into the test section in the form of a sheet beam through a spherical and a cylindrical lens. To seed the flow, hollow glass spheres of 10 μm in diameter are inserted into the flow. Particle image pairs are captured by a high-speed CCD camera (SVSI), which is synchronized with the laser pulses. To calculate velocity vector from the particle images, a cross-correlation algorithm [12] based on FFT (fast Fourier transform) is applied. The interrogation windows with 16 x 16 pixels are overlapped as much as 50%. In addition, window shifting and recursive correlation techniques [13] are applied to enhance the signal-to-noise ratio. A total of 800 instantaneous velocity fields for each water depth are acquired to calculate the time-averaged and fluctuating velocity vectors.

3. Results and Discussion

For the two-dimensional open channel (width-to-depth ratio > 10), it is known that the maximum velocity is located at the free surface [6]. Whereas, it is not always true in the circular open channel since the effect of side wall propagates into the middle of the discharging area. Fig. 3 shows the time-averaged velocity profiles when the water depth varies from 30 – 80% of the pipe diameter. To characterize the velocity profile, the measured data are least-squares fitted to the following velocity distribution function proposed by Chiu and his group [6-8] for the arbitrary-shaped open channel flow.

$$\xi = Y\exp(1-Y) \tag{1}$$

$$\frac{u(\xi)}{u_{\max}} = \frac{1}{M}\ln\left[1+(e^{M}-1)\frac{\xi-\xi_0}{\xi_{\max}-\xi_0}\right] \tag{2}$$

$$\frac{\bar{u}}{u_{\max}} = \frac{e^{M}}{e^{M}-1} - \frac{1}{M} \tag{3}$$

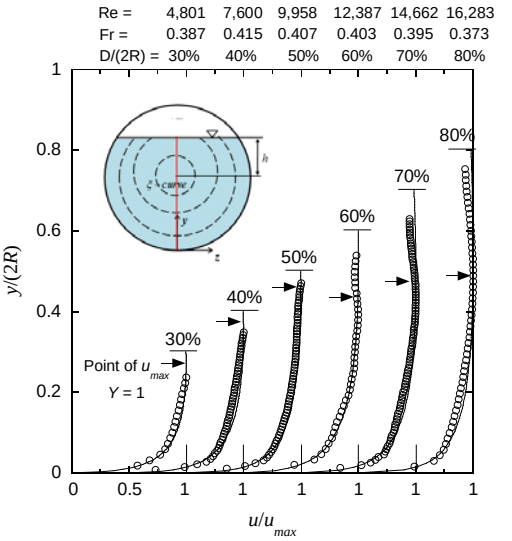

Figure 3: Mean velocity profiles according to the water depth. The circular symbols denote the PIV measurement data and the solid lines are the least-squares fitted function given in equation (2). The arrows mark the point of maximum velocity.

where $Y = y/(D-h)$ D is the water depth and h is the distance measured from the free surface to the point of maximum velocity. If $h > 0$, the maximum velocity occurs below the free surface. If $h \leq 0$, the velocity gradient is always positive and the maximum velocity occurs on the free surface. The velocity u is expressed as a function of a curvilinear coordinate system ξ. $\bar{u}$ and $u_{\max}$ are the mean and maximum values of $u(\xi)$, respectively. ξ_0 and $\xi_{\max}$ are the minimum and maximum values of ξ at which u is zero and maximum, respectively. M is a parameter. As dimensionless numbers, Reynolds and Froude numbers are defined as $\mathrm{Re} = 4\bar{u}R_h/\nu$ and $\mathrm{Fr} = \bar{u}/\sqrt{gD_m}$, respectively, where ν is the kinematic viscosity, g is the gravitational acceleration, D_m is the hydraulic depth defined as the wet area divided by the width of the free surface. These dimensionless numbers are listed in Fig. 3. The point of maximum velocity (D-h) is located just

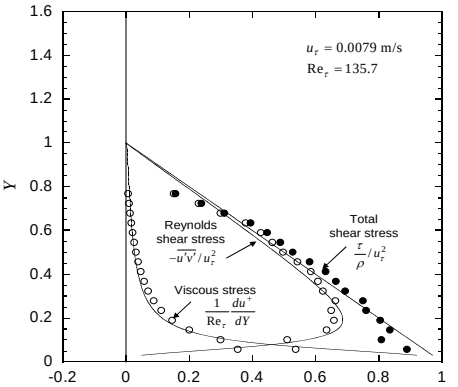

(a) Water depth = 30%

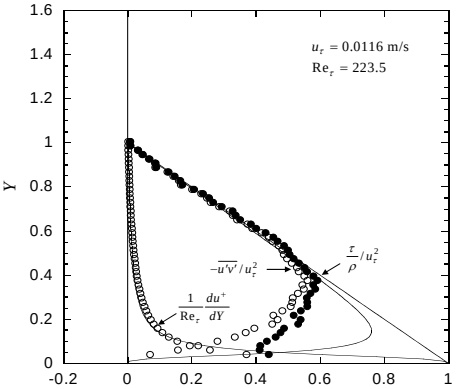

(b) Water depth = 40%

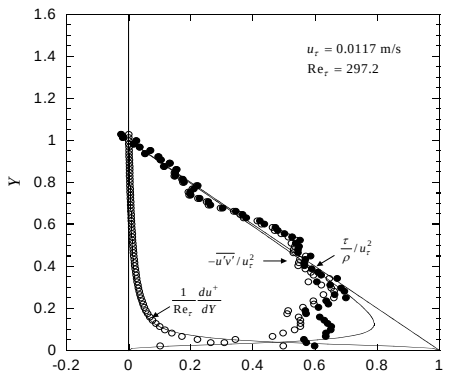

(c) Water depth = 50%

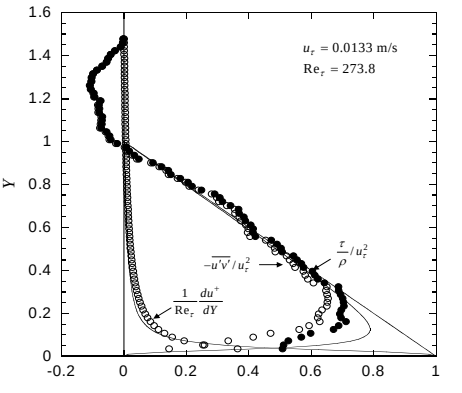

(d) Water depth = 60%

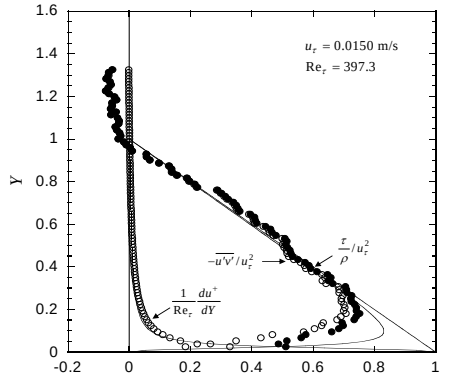

(e) Water depth = 70%

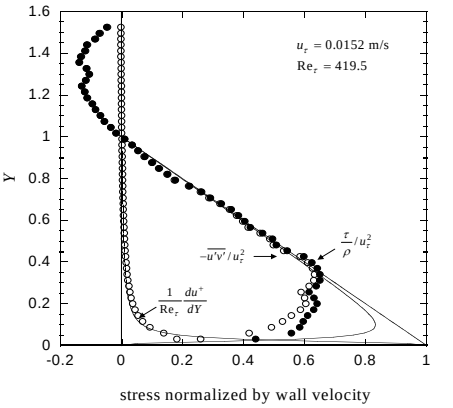

(f) Water depth = 80%

Figure 4: Distribution of turbulent shear stresses according to the water depth. The circular open and filled symbols denote the PIV measurement data and the solid lines are the theoretical curves based upon the Prandtl's mixing length theory and van Driest's damping function.

below the free surface if the water depth is lower than 50%. On the other hand, it is fixed near the channel center for the higher water depth than 50% since the side wall affect more significantly the flow near the free surface.

Figure 4 shows the distributions of turbulent shear stresses for various water depths. The friction velocity u_τ is used to normalize the stresses. Since it is difficult to measure the wall friction directly, it is determined from the extrapolation of the linear profile of the total shear stress τ in equation (4) to the wall.

$$\frac{\tau}{\rho} \equiv -\overline{u'v'} + \nu\frac{du}{dy} = u_\tau^2(1-Y) \tag{4}$$

In the above equation, the first term in the right-hand side is the Reynolds shear stress and the second term is the viscous stress. From the PIV measurement data, the Reynolds shear stress can be obtained by multiplying the fluctuating velocity components u' and v'. The velocity gradient in the second term is evaluated by differentiating the velocity distribution function in equation (2). The summation of these two terms yields the total shear stress which is related to the friction velocity in the last term of equation (4). Here, the coordinate is non-dimensionalized by the position of maximum velocity, so that Y is 1 at the point of maximum velocity and 0 at the wall. In the fully-developed, two-dimensional turbulent flow, the Reynolds shear stress can be modeled with the help of the Prandtl's mixing length theory and van Driest's damping function [14] as follows;

$$\frac{du^+}{dY} = \frac{2\,\mathrm{Re}_\tau(1-Y)}{1+\sqrt{1+4l^{+2}(1-Y)}} \tag{5}$$

$$l^+ = \kappa y^+ \Gamma \tag{6}$$

$$\Gamma = 1-\exp\left(-\frac{y^+}{B}\right) \tag{7}$$

in which $\mathrm{Re}_\tau = u_\tau(D\text{-}h)/\nu$, $u^+ = u/u_\tau$ and $y^+ = yu_\tau/\nu$. κ is the von Karman constant and B an empirical constant (=26). Figure 4 shows that the theoretical viscous stress $1/\mathrm{Re}_\tau du^+/dY$ calculated from equation (5) agrees well with the experimental data. In the near-wall region, however, the measured Reynolds shear stress has lower values than the theoretical estimation, which makes the total shear deviate from the linear function. The reason for these deviations in the circular open channel flow is not clear in the present study. It should be noted that the theoretical functions are based upon the assumption of two-dimensional turbulent boundary layer. Nevertheless, the most significant finding in this figure is that the Reynolds shear stress yields different distributions in the outer region according to the variation of water depth. For the lower water depth than 50%, the linear profile of the Reynolds shear stress extends to the free surface. However, for the higher water depth than 50%, it becomes negative over the point of maximum velocity and then it approaches 0 at the free surface.

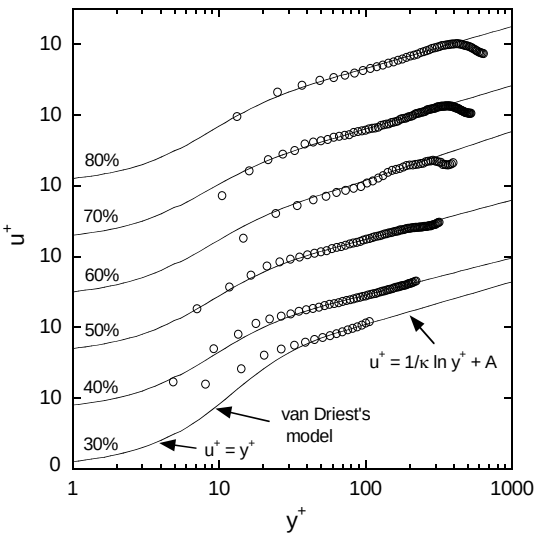

Figure 5: Comparison of the measured mean velocity with the log law of turbulent boundary layer

In Fig. 5, the mean velocity is plotted in wall unit and compared with the law of the wall ($u^+ = 1/\kappa \ln y^+ + A$). From a linear regression analysis, the von Karman constant κ and the integral constant A are obtained. Inside the viscous sublayer ($y^+ < 5$), laminar shearing stress governs the flow ($u^+ = y^+$). In the buffer layer ($5 < y^+ < 70$), laminar and turbulent frictionsare of the same order of magnitude and the analytic curves in Fig. 5 are calculated by the Prandtl's mixing length theory and van Driest's damping function in equation (5). In the wall region ($y^+ < 300$), the present data agree well with the universal velocity distribution of the log law. However, if the water depth goes up higher than 50%, the mean velocity in the wake region ($y^+ > 300$) deviates from the standard log law of turbulent boundary layer, which is not observed at the lower water depth than 50%. The deviation of the mean velocity from the log law might be explained by the concept of the Coles's wake function [14], but more systematic analysis is required in further studies to correlate the amount of deviation to the influence of side wall.

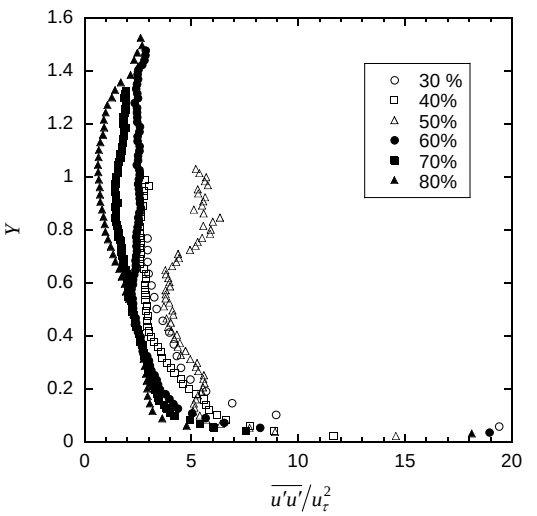

Figure 6: Streamwise Reynolds normal stress according to the variation of water depth.

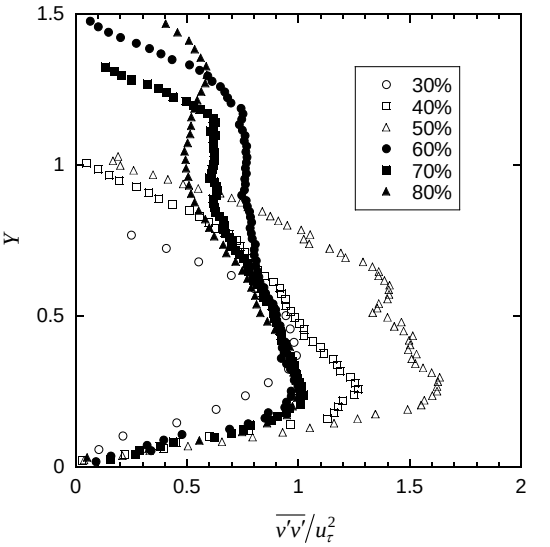

Figure 7: Cross-stream Reynolds normal stress according to the variation of water depth.

In Figures 6-7, the Reynolds normal stresses normalized by the friction velocity are plotted according to the variation of water depth. The streamwise component as shown in Fig. 6 decreases exponentially as the vertical position goes far from the wall. With regard to the variation of water depth, there is no significant difference even though the values at the lower water depths are a little bit larger than those at the higher water depths. On the other hand, the cross-stream component as shown in Fig. 7 has a different behavior when the water depth varies. If the water depth is lower than 50%, its peak value in the near-wall region increases with water depth, and then it decreases sharply in the outer region. If the water depth exceeds 50%, the peak values are almost the same, not affected by the change of water depth. As the position further goes up, it shows a slight decrease in the outer region and a sharp decrease near the free surface.

4. Conclusions

In the present study, turbulent flows in a

circular open channel have been measured by a PIV system. For a fixed channel slope, different turbulence characteristics were shown whether the water depth is higher than 50% of a pipe diameter or not. When the water depth goes up higher than 50%, the point of maximum velocity is fixed near the pipe center, while at the lower water depth than 50%, it increases with the water depth but remains near the free surface. The Reynolds shear stress at the lower water depth follows the two-dimensional turbulent boundary layer except in the near-wall region. At the higher water depth, the Reynolds shear stress becomes negative above the point of maximum velocity and it approaches 0 at the free surface. In addition, the mean velocity considerably deviates from the standard log law in the region above the point of maximum velocity. With regard to the Reynolds normal stress, at the lower water depth than 50%, the peak value of its cross-stream component shows an increase with the water depth, accompanying with a sharp decrease in the outer region. At the higher water depth, however, the peak value is not changed by the variation of the water depth, accompanying with a slight decrease in the outer region and a sharp decrease near the free surface.

References

[1] Blinco P.H. and Partheniades E., “Turbulence characteristics in free surface flows over smooth and rough boundaries”, J. Hydraulic Res., vol. 9, pp. 43-69, 1971.

[2] Nakagawa H. and NezuI., “Structure of space-time correlation of bursting phenomena in an open channel flow”, J. Fluid Mech., vol. 104, pp. 1-43, 1981.

[3] Nezu I. and Rodi W., “Open-channel flow measurements with a laser Doppler anemometer”, J. Hydraulic Engrg., vol. 112, no. 5, pp. 335-355, 1986.

[4] Kirkgoz M.S., “Turbulent velocity profiles for smooth and rough open channel flow”, J. Hydraulic Engrg., vol. 115, no. 11, pp. 1543-1561, 1989.

[5] Grass A.J., “Structural features of turbulent flow over smooth and rough boundaries”, J. Fluid Mech., vol. 50, pp. 233-255, 1971.

[6] Chiu C.L., “Velocity distribution in open channel flow”, J. Hydraulic Engrg., vol. 115, no. 5, pp. 576-594, 1989.

[7] Chiu C.L. and Murray D.W., “Variation of velocity distribution along nonuniform open-channel flow”, J. Hydraulic Engrg., vol. 118, no. 7, pp. 989-1001, 1992.

[8] Chiu C.L. and Said C.A.A., “Maximum and mean velocities and entropy in open-channel flow”, J. Hydraulic Engrg., vol. 121, no. 1, pp. 26-35, 1995.

[9] Keane R.D. and Adrian R.J., “Theory of cross-correlation analysis of PIV images”, Appl. Sci. Res., vol. 49, pp. 191-215, 1992.

[10] Doorne C.W.H. and Westerweel J., “Measurement of laminar, transitional and turbulent pipe flow using stereoscopic-PIV”, Exp. Fluids, vol. 42, no. 2, pp. 259-279, 2007.

[11] Sung J., Yoon J.-I. and Lee M.H., “Effect of water depth on three-dimensional velocity distributions inside a partially filled circular pipe”, Proc. 7th PSFVIP, Kaosiung, Taiwan, P-008, pp. 1-5, 2009.

[12] Sung J. and Yoo J.Y., “Three-dimensional phase averaging of time-resolved PIV measurement data”, Meas. Sci. Technol., vol. 12, no. 6, pp. 655-662, 2001.

[13] Scarano F. and Riethmuller M.L., “Iterative multigrid approach in PIV image processing with discrete window offset”, Exp. Fluids, vol. 26, no. 6, pp. 513-523, 1999.

[14] Schlichting H., “Boundary layer theory”, 7th edition, McGraw-Hill, 1979.

Author Profile

Sun-Gu Kim

He received his B.S. degree in Mechanical Engineering from Seoul National University of Science and Technology in 2011. He then has been a graduate student of Department of Mechanical Engineering in Seoul National University of Science and Technology

Jae-Yong Sung

He received his B.S. degree in Mechanical Engineering from Seoul National University in 1994. He then received the M.Eng. and Ph.D degrees in School of Mechanical and Aerospace Engineering from Seoul National University in 1996 and 2001. Since 2004, he has been a professor of Department of Mechanical Engineering in Seoul National University of Science and Technology.

Myeong-Ho Lee

He received his B.S. degree in Mechanical Engineering from Kyung-Hee University in 1984. He then received the M.Eng. and Ph.D degrees in Department of Mechanical Engineering from Kyung-Hee University in 1986 and 1993. Since 1993, he has been a professor of Department of Mechanical Engineering in Seoul National University of Science and Technology.